

NONDEGENERATE FERMIONS IN THE BACKGROUND OF THE SPHALERON BARRIER

Guido Nolte

Fachbereich Physik, Universität Oldenburg, Postfach 2503
D-26111 Oldenburg, Germany

Jutta Kunz

Fachbereich Physik, Universität Oldenburg, Postfach 2503
D-26111 Oldenburg, Germany

and

Instituut voor Theoretische Fysica, Rijksuniversiteit te Utrecht
NL-3508 TA Utrecht, The Netherlands

Burkhard Kleihaus

Fachbereich Physik, Universität Oldenburg, Postfach 2503
D-26111 Oldenburg, Germany

May 10, 2018

Abstract

We consider level crossing in the background of the sphaleron barrier for nondegenerate fermions. The mass splitting within the fermion doublets allows only for an axially symmetric ansatz for the fermion fields. In the background of the sphaleron we solve the partial differential equations for the fermion functions. We find little angular dependence for our choice of ansatz. We therefore propose a good approximate ansatz with radial functions only. We generalize this approximate ansatz with radial functions only to fermions in the background of the sphaleron barrier and argue, that it is a good approximation there, too.

1 Introduction

The explanation of the observed baryon asymmetry of the universe represents a challenging problem. Although far from solving this highly complex problem, we know at least what features a theory must have to allow for an explanation. It is therefore remarkable that the standard model fulfills all three Sakharov-conditions to generate the observed baryon asymmetry: C and CP violation, a first order phase transition and non-conservation of baryon number [1].

Here we are concerned with the violation of baryon number (or more generally fermion number) in the standard model. It was discovered by 't Hooft [2] as a consequence of the Adler-Bell-Jackiw anomaly present in chiral gauge theories. In particular 't Hooft studied the fermion number violation induced by vacuum to vacuum tunneling processes described by instantons, resulting in extremely small tunneling rates.

In Weinberg-Salam theory topologically distinct vacua are separated by finite energy barriers. The height of the barriers is given by the energy of the sphaleron, an unstable solution of the static field equations [3, 4]. Thus the sphaleron determines the minimal energy needed for a classically allowed vacuum to vacuum transition. The probability for a transition is expected to be enhanced significantly, if enough energy is put into the system under consideration, either in suitable (future) accelerators or at high temperatures in the early universe [5-10].

While the barrier is traversed baryon number violation may be seen explicitly by analyzing the corresponding Dirac equation in the bosonic background fields. The lowest positive energy continuum state becomes continuously deformed along the barrier until it reaches the negative energy continuum, passing zero energy precisely at the top of the energy barrier, at the sphaleron [11-15]. Investigating the whole spectrum of the Dirac equation shows, that along the barrier in fact all levels become continuously deformed into the next lower levels, resulting finally in an identical spectrum, where only the number of occupied levels above the Dirac sea has decreased by one [16].

These calculations [11-16] are based on the approximation, that the fermion doublets are degenerate in mass (and that the Weinberg angle may be set to zero [17, 18]), allowing for a spherically symmetric ansatz for the fermion wave function. For the physical situation of highly nondegenerate fermion masses (at least for the heavy flavours) an analogous calculation is far more involved, since the spherically symmetric ansatz fails and the equations of motion cannot be reduced to ordinary differential equations. (This is in contrast to the case of instantons [19].)

Here we consider an axially symmetric ansatz for the fermion fields in the background of the sphaleron barrier. The ansatz is chosen in such a way, that it is “almost spherically symmetric”, in the sense that the functions involved have little angular dependence. Due to the symmetry of the sphaleron the ansatz simplifies considerably in the background field of the sphaleron. In this case we solve numerically the full set of partial differential equations for the fermion functions. We then consider a set of approximate ordinary differential equations for the fermion functions, finding almost identical solutions. Because

of the numerical complexity involved in solving the full set of partial differential equations in the background of the sphaleron barrier, we consider in this general case only an approximate set of ordinary differential equations for radial fermion functions. We argue that these equations represent a good approximation as well.

In section 2 we briefly review the Weinberg-Salam Lagrangian (for vanishing mixing angle) for nondegenerate fermion doublets. In section 3 we present our axially symmetric ansatz for the fermions, constructed as a generalization of the usual spherically symmetric ansatz. In section 4 we consider fermions in the background of the sphaleron. We derive the equations of motion, present the solutions of the full set of partial differential equations, and compare with the solutions of the set of approximate ordinary differential equations. In section 5 we consider fermions in the background of the sphaleron barrier. We present our conclusions in section 6.

2 Weinberg-Salam Lagrangian

We start with the bosonic sector of the Weinberg-Salam theory in the limit of vanishing Weinberg angle, where the electromagnetic field decouples and can be set to zero,

$$\mathcal{L}_b = -\frac{1}{4}F_{\mu\nu}^a F^{\mu\nu,a} + (D_\mu\Phi)^\dagger(D^\mu\Phi) - \lambda(\Phi^\dagger\Phi - \frac{1}{2}v^2)^2 \quad (1)$$

with the field strength tensor

$$F_{\mu\nu}^a = \partial_\mu V_\nu^a - \partial_\nu V_\mu^a + g\epsilon^{abc}V_\mu^b V_\nu^c, \quad (2)$$

and the covariant derivative

$$D_\mu = \partial_\mu - \frac{1}{2}ig\tau^a V_\mu^a. \quad (3)$$

The $SU(2)_L$ gauge symmetry is spontaneously broken due to the non-vanishing vacuum expectation value v of the Higgs field

$$\langle\Phi\rangle = \frac{v}{\sqrt{2}} \begin{pmatrix} 0 \\ 1 \end{pmatrix}, \quad (4)$$

leading to the boson masses

$$M_W = M_Z = \frac{1}{2}gv, \quad M_H = v\sqrt{2\lambda}. \quad (5)$$

We employ the values $M_W = 80$ GeV, $g = 0.65$.

For vanishing mixing angle, considering only one fermion doublet, the fermion Lagrangian reads

$$\begin{aligned} \mathcal{L}_f &= \bar{q}_L i\gamma^\mu D_\mu q_L + \bar{q}_R i\gamma^\mu \partial_\mu q_R \\ &- f^{(u)}(\bar{q}_L \tilde{\Phi} u_R + \bar{u}_R \tilde{\Phi}^\dagger q_L) - f^{(d)}(\bar{d}_R \Phi^\dagger q_L + \bar{q}_L \Phi d_R), \end{aligned} \quad (6)$$

where q_L denotes the lefthanded doublet (u_L, d_L) , while q_R abbreviates the righthanded singlets (u_R, d_R) , with $\tilde{\Phi} = i\tau_2\Phi^*$. The fermion masses are given by

$$M_{u,d} = \frac{1}{\sqrt{2}} f^{(u,d)} v . \quad (7)$$

The fermion equations read in dimensionless coordinates (chosen in units of M_W)

$$(i\frac{\partial}{\partial t} + i\sigma^i \frac{\partial}{\partial x^i} + \frac{1}{2}\tau^a V_i^a \sigma^i) q_L - (mM + \Delta m M \tau_z) q_R = 0 \quad (8)$$

and

$$(i\frac{\partial}{\partial t} - i\sigma^i \frac{\partial}{\partial x^i}) q_R - (mM^\dagger + \Delta m \tau_z M^\dagger) q_L = 0 , \quad (9)$$

where M is the Higgsfield matrix defined by

$$\Phi = \frac{v}{\sqrt{2}} M \begin{pmatrix} 0 \\ 1 \end{pmatrix} , \quad (10)$$

and m and Δm are the average fermion mass and half the mass difference (in units of M_W)

$$m = (M_u + M_d)/(2M_W) , \quad (11)$$

$$\Delta m = (M_u - M_d)/(2M_W) . \quad (12)$$

3 Ansatz

For the gauge and Higgs fields along the sphaleron barrier we take the usual spherically symmetric ansatz in the temporal gauge

$$V_i^a = \frac{1 - f_A(r)}{gr} \varepsilon_{aij} \hat{r}_j + \frac{f_B(r)}{gr} (\delta_{ia} - \hat{r}_i \hat{r}_a) + \frac{f_C(r)}{gr} \hat{r}_i \hat{r}_a , \quad (13)$$

$$V_0^a = 0 , \quad (14)$$

$$\Phi = \frac{v}{\sqrt{2}} (H(r) + i\vec{\tau} \cdot \hat{r} K(r)) \begin{pmatrix} 0 \\ 1 \end{pmatrix} . \quad (15)$$

Due to a residual gauge degree of freedom we are free to choose the gauge $f_C = 0$.

To construct an appropriate ansatz for nondegenerate fermions we begin by recalling the spherically symmetric ansatz for degenerate fermions with $\Delta m = 0$ [11-16,20], containing four radial functions,

$$q_L(\vec{r}, t) = e^{-i\omega t} M_W^{\frac{3}{2}} [G_L(r) + i\vec{\sigma} \cdot \hat{r} F_L(r)] \chi_h , \quad (16)$$

$$q_R(\vec{r}, t) = e^{-i\omega t} M_W^{\frac{3}{2}} [G_R(r) + i\vec{\sigma} \cdot \hat{r} F_R(r)] \chi_h , \quad (17)$$

where the normalized hedgehog spinor χ_h satisfies the spin-isospin relation

$$\vec{\sigma}\chi_h + \vec{\tau}\chi_h = 0. \quad (18)$$

The generalized axially symmetric ansatz contains the spherically symmetric ansatz, where the four functions G_L , F_L , G_R and F_R now depend on the variables r and θ . Because of the presence of the τ_z -terms in the field equations (8)-(9) for $\Delta m \neq 0$, we need to ‘double’ the ansatz by adding terms of the same structure, but with χ_h replaced by $\tau_z\chi_h$, involving the four new (r and θ -dependent) functions ΔG_L , ΔF_L , ΔG_R and ΔF_R . The ansatz now contains eight functions, which are in general complex and θ -dependent, caused by various occurrences of the nonvanishing anticommutator $[\vec{\tau} \cdot \hat{r}, \tau_z]_+ = 2\cos\theta$ in the equations of motion. Considering the θ -dependence of the functions, the real part is even in $\cos\theta$ while the imaginary part is odd. This then suggests the following parametrization of the general axially symmetric ansatz, involving 16 real functions of the variables r and $p = \cos^2\theta$,

$$\begin{aligned} q_L(\vec{r}, t) = & e^{-i\omega t} M_W^{\frac{3}{2}} \left([G_L^1(r, p) + i\cos(\theta)G_L^2(r, p) + i\vec{\sigma} \cdot \hat{r}(F_L^1(r, p) + i\cos(\theta)F_L^2(r, p))] \right. \\ & + \tau_z[\Delta G_L^1(r, p) + i\cos(\theta)\Delta G_L^2(r, p) \\ & \left. + i\vec{\sigma} \cdot \hat{r}(\Delta F_L^1(r, p) + i\cos(\theta)\Delta F_L^2(r, p))] \right) \chi_h, \end{aligned} \quad (19)$$

$$\begin{aligned} q_R(\vec{r}, t) = & e^{-i\omega t} M_W^{\frac{3}{2}} \left([G_R^1(r, p) + i\cos(\theta)G_R^2(r, p) + i\vec{\sigma} \cdot \hat{r}(F_R^1(r, p) + i\cos(\theta)F_R^2(r, p))] \right. \\ & + \tau_z[\Delta G_R^1(r, p) + i\cos(\theta)\Delta G_R^2(r, p) \\ & \left. + i\vec{\sigma} \cdot \hat{r}(\Delta F_R^1(r, p) + i\cos(\theta)\Delta F_R^2(r, p))] \right) \chi_h. \end{aligned} \quad (20)$$

The choice of ansatz (19)-(20) is not unique. We have also considered alternative parametrizations of the axially symmetric fermion ansatz. These involve different fermion functions, uniquely related to the above fermion functions. The crucial advantage of the ansatz (19)-(20) lies in the observation, that its fermion functions have only a very weak angular dependence in the background field of the sphaleron, as shown below. This is in contrast to the alternative parametrizations considered.

4 Sphaleron

We first consider fermions in the background of the sphaleron. Since the background field barrier is symmetric about the sphaleron, the fermion eigenvalue is precisely zero at the sphaleron [11-16], also for nondegenerate fermion masses. As for degenerate fermion masses, the fermion ansatz (19)-(20) then simplifies significantly in the background field of the sphaleron. This is due to the parity reflection symmetry of the sphaleron, for which the functions f_B and H vanish, resulting in the decoupling of eight of the 16 functions. These functions, F_L^1 , G_L^2 , ΔF_L^1 , ΔG_L^2 and F_R^1 , G_R^2 , ΔF_R^1 , ΔG_R^2 , can therefore consistently

be set to zero. After dropping the number index on the remaining eight functions the set of partial differential equations in the variables r and p reads

$$0 = -G_R' + \frac{2}{r}p\frac{\partial}{\partial p}G_R + \frac{1}{r}(1 + 2p\frac{\partial}{\partial p})\Delta F_R - mKG_L + \Delta mK\Delta G_L - 2pKm\Delta F_L, \quad (21)$$

$$0 = -\Delta G_R' + \frac{1}{r}(1 + 2p\frac{\partial}{\partial p})F_R + \frac{2}{r}p\frac{\partial}{\partial p}\Delta G_R + mK\Delta G_L - \Delta mKG_L - 2pK\Delta m\Delta F_L, \quad (22)$$

$$0 = F_R' + \frac{1}{r}(3 + 2p\frac{\partial}{\partial p})F_R + \frac{2}{r}\frac{\partial}{\partial p}\Delta G_R - \Delta mK\Delta F_L + mK(F_L + 2\Delta G_L), \quad (23)$$

$$0 = \Delta F_R' + \frac{1}{r}(3 + 2p\frac{\partial}{\partial p})\Delta F_R + \frac{2}{r}\frac{\partial}{\partial p}G_R - mK\Delta F_L + \Delta mK(F_L + 2\Delta G_L), \quad (24)$$

$$0 = G_L' - \frac{2}{r}p\frac{\partial}{\partial p}G_L - \frac{1}{r}(1 + 2p\frac{\partial}{\partial p})\Delta F_L + mKG_R + \Delta mK\Delta G_R + 2pK(m\Delta F_R + \Delta mF_R) + \frac{1-f_A}{r}(G_L + p\Delta F_L), \quad (25)$$

$$0 = \Delta G_L' - \frac{2}{r}p\frac{\partial}{\partial p}\Delta G_L - \frac{1}{r}(1 + 2p\frac{\partial}{\partial p})F_L - K(m\Delta G_R + \Delta mG_R), \quad (26)$$

$$0 = -F_L' - \frac{1}{r}(3 + 2p\frac{\partial}{\partial p})F_L - \frac{2}{r}\frac{\partial}{\partial p}\Delta G_L - mKF_R - \Delta mK\Delta F_R - 2K(m\Delta G_R + \Delta mG_R) + \frac{1-f_A}{r}(F_L + \Delta G_L), \quad (27)$$

$$0 = -\Delta F_L' - \frac{1}{r}(3 + 2p\frac{\partial}{\partial p})\Delta F_L - \frac{2}{r}\frac{\partial}{\partial p}G_L + \Delta mKF_R + mK\Delta F_R. \quad (28)$$

Inspection of the equations shows, that only three equations, eqs. (21),(22) and (25), contain p -dependent terms, when the terms involving the partial derivative with respect to p , present in all eight equations, are not considered. In fact only three functions occur with a prefactor p . These are F_R , ΔF_R and ΔF_L . If these three functions are small, then the ansatz is approximately spherically symmetric in the sense, that all functions have little angular dependence. In the following we show, that this is indeed the case.

Let us denote the three functions F_R , ΔF_R and ΔF_L as b , as ‘bad’ functions, and the other five functions as g , as ‘good’ functions. First we note, that we could set all three bad functions b consistently equal to zero, if the source term

$$s = -K(F_L + 2\Delta G_L) \quad (29)$$

for the bad functions F_R and ΔF_R in eqs. (23) and (24) did vanish. Then the five good functions g were pure radial functions. Let us therefore inspect this source term more closely and split it into two terms, $s = a_1 - a_2$, with

$$a_1 = -KF_L, \quad (30)$$

and

$$a_2 = 2K\Delta G_L . \quad (31)$$

If $a_1 = a_2$, the source term vanishes. We now argue that a_1 and a_2 are approximately equal. Setting the bad functions $F_R, \Delta F_R$ and ΔF_L equal to zero, and neglecting terms with prefactors $\frac{1}{r}$, for large r eqs. (26) and (27) reduce to

$$\Delta G_L' = K(m\Delta G_R + \Delta m G_R) ,$$

and

$$F_L' = -2K(m\Delta G_R + \Delta m G_R) .$$

With the proper boundary conditions at infinity we thus find for large r for the solutions the desired behaviour, $F_L = -2\Delta G_L$, i.e. the source term vanishes there. On the other hand, for small r the source term vanishes, since the function K vanishes. In the intermediate region the size of the source term needs numerical analysis.

We have solved the set of partial differential equations in the background of the sphaleron numerically for various values of the average mass m and the mass difference Δm . Let us consider a typical numerical result. In Fig. 1 we show the ‘good’ lefthanded functions, $G_L, \Delta G_L$ and F_L , with normalization $G_L(0) = 1$, for three values of the angle θ ($\theta = 0, \pi/4$ and $\pi/2$) for the mass parameters $m = 0.5$ and $\Delta m = 0.25$. The θ -dependence of the functions is too small to be seen in the figure, being on the order of 10^{-4} . The corresponding bad lefthanded function ΔF_L is very small, indeed. For the case considered it is less than $5 \cdot 10^{-4}$, i.e. two orders of magnitude smaller than the good functions, with almost no θ -dependence at all.

These results suggest to approximate all functions by radial functions. We have therefore obtained a new set of ordinary differential equations by integrating out the θ -dependence in the energy density, before variation with respect to the fermion functions. The resulting equations then differ only in prefactors for the three bad functions, apart from the absence of the partial derivatives with respect to p . In block form the approximate set of differential equations reads

$$\begin{pmatrix} g' \\ b' \end{pmatrix} = \begin{pmatrix} A & B \\ C & D \end{pmatrix} \begin{pmatrix} g \\ b \end{pmatrix} , \quad (32)$$

where A is a 5 by 5 matrix, B is a 5 by 3 matrix etc. The vector Cg represents the source terms of the good functions g for the bad functions b . (It is identical in both sets of equations.) These source terms are $ms, \Delta ms$ and zero for $F_R, \Delta F_R$ and ΔF_L , respectively, with the source s defined in eq. (29).

Solving the approximate set of ordinary differential equations leads to results almost identical to those of the full partial differential equations. This is demonstrated in Fig. 1, where also the approximate good lefthanded functions $G_L, \Delta G_L$ and F_L , with normalization $G_L(0) = 1$, are shown. The difference of the approximate functions and the exact functions is too small to be seen in the figure, being on the order of 10^{-3} . The bad lefthanded function ΔF_L is less than 10^{-4} .

Thus the exact calculation and the radial approximation result in almost identical results, and the bad functions are very small, indeed. We are therefore free to present in the following only results obtained with the approximate calculation. In Figs. 2-4 we show the same good lefthanded functions, G_L , ΔG_L and F_L , as in Fig. 1 for the same value of the average mass $m = 0.5$, but for three different values of the mass difference, $\Delta m = 0.25$, 0.5, and 0.75. Fig. 5 is the corresponding figure for the good righthanded function G_R . The functions G_L and G_R are the only functions which do not vanish in the limit $\Delta m = 0$. All other functions, which vanish for $\Delta m = 0$, are approximately proportional to Δm as seen in Figs. 3 and 4. Finally in Fig. 6 we demonstrate the approximate cancellation of the source terms a_1 and a_2 , responsible for the fact that the bad functions are very small.

5 Sphaleron Barrier

Let us now consider nondegenerate fermions in the background of the sphaleron barrier. Along the barrier we expect a smooth transition of one fermion level from the positive continuum to the negative continuum. In the case of degenerate fermion masses, all fermion levels change along the barrier to the respective next lower level [16], thus only one level crosses zero, and the spectrum exhibits no crossing of any two levels. Expecting the same qualitative behaviour of the spectrum in the case of nondegenerate masses, the lowest free fermion level, corresponding to the lower mass fermion of the doublet, then should cross zero.

In the general background of the sphaleron barrier the full ansatz, eqs. (19)-(20), is needed. The background fields along the barrier may be taken from the extremal path calculations [15] or, as done here, from the gradient approach [20]. The set of partial equations for the 16 real fermionic functions of the variables r and p reads

$$0 = \omega F_R^1 - G_R^{1'} + \frac{2}{r} p \frac{\partial}{\partial p} G_R^1 + \frac{1}{r} (1 + 2p \frac{\partial}{\partial p}) \Delta F_R^2 - m(K G_L^1 + H F_L^1) - \Delta m(-K \Delta G_L^1 + H \Delta F_L^1) - 2p K m \Delta F_L^2, \quad (33)$$

$$0 = \omega F_R^2 - G_R^{2'} + \frac{1}{r} (1 + 2p \frac{\partial}{\partial p}) G_R^2 - \frac{2}{r} \frac{\partial}{\partial p} \Delta F_R^1 - \Delta m(-K \Delta G_L^2 + H \Delta F_L^2) - m(K G_L^2 + H F_L^2 - 2K \Delta F_L^1), \quad (34)$$

$$0 = \omega \Delta F_R^1 - \Delta G_R^{1'} + \frac{1}{r} (1 + 2p \frac{\partial}{\partial p}) F_R^2 + \frac{2}{r} p \frac{\partial}{\partial p} \Delta G_R^1 - m(-K \Delta G_L^1 + H \Delta F_L^1) - \Delta m(K G_L^1 + H F_L^1) - 2p K \Delta m \Delta F_L^2, \quad (35)$$

$$0 = \omega \Delta F_R^2 - \Delta G_R^{2'} + \frac{1}{r} (1 + 2p \frac{\partial}{\partial p}) \Delta G_R^2 - \frac{2}{r} \frac{\partial}{\partial p} F_R^1 - m(-K \Delta G_L^2 + H \Delta F_L^2) - \Delta m(K G_L^2 + H F_L^2 - 2K \Delta F_L^1), \quad (36)$$

$$0 = \omega G_R^1 + F_R^{1'} + \frac{1}{r} (2 + 2p \frac{\partial}{\partial p}) F_R^1 - \frac{1}{r} (1 + 2p \frac{\partial}{\partial p}) \Delta G_R^2 - m(H G_L^1 - K F_L^1) - \Delta m(H \Delta G_L^1 + K \Delta F_L^1) - 2p K m \Delta G_L^2, \quad (37)$$

$$0 = \omega G_R^2 + F_R^{2'} + \frac{1}{r}(3 + 2p\frac{\partial}{\partial p})F_R^2 + \frac{2}{r}\frac{\partial}{\partial p}\Delta G_R^1 - \Delta m(H\Delta G_L^2 + K\Delta F_L^2) - m(HG_L^2 - KF_L^2 - 2K\Delta G_L^1), \quad (38)$$

$$0 = \omega\Delta G_R^1 + \Delta F_R^{1'} + \frac{1}{r}(2 + 2p\frac{\partial}{\partial p})\Delta F_R^1 - \frac{1}{r}(1 + 2p\frac{\partial}{\partial p})G_R^2 - \Delta m(HG_L^1 - KF_L^1) - m(H\Delta G_L^1 + K\Delta F_L^1) - 2pK\Delta m\Delta G_L^2, \quad (39)$$

$$0 = \omega\Delta G_R^2 + \Delta F_R^{2'} + \frac{1}{r}(3 + 2p\frac{\partial}{\partial p})\Delta F_R^2 + \frac{2}{r}\frac{\partial}{\partial p}G_R^1 - m(H\Delta G_L^2 + K\Delta F_L^2) - \Delta m(HG_L^2 - KF_L^2 - 2K\Delta G_L^1), \quad (40)$$

$$0 = \omega F_L^1 + G_L^{1'} - \frac{2}{r}p\frac{\partial}{\partial p}G_L^1 - \frac{1}{r}(1 + 2p\frac{\partial}{\partial p})\Delta F_L^2 + m(KG_R^1 - HF_R^1) + \Delta m(K\Delta G_R^1 - H\Delta F_R^1) + 2pK(m\Delta F_R^2 + \Delta mF_R^2) + \frac{1-f_A}{r}(G_L^1 + p\Delta F_L^2) + \frac{f_B}{r}(F_L^1 - p\Delta G_L^2), \quad (41)$$

$$0 = \omega F_L^2 + G_L^{2'} - \frac{1}{r}(1 + 2p\frac{\partial}{\partial p})G_L^2 + \frac{2}{r}\frac{\partial}{\partial p}\Delta F_L^1 + m(KG_R^2 - HF_R^2) + \Delta m(K\Delta G_R^2 - H\Delta F_R^2) - 2K(m\Delta F_R^1 + \Delta mF_R^1) + \frac{1-f_A}{r}(G_L^2 - \Delta F_L^1) + \frac{f_B}{r}(F_L^2 + \Delta G_L^1), \quad (42)$$

$$0 = \omega\Delta F_L^1 + \Delta G_L^{1'} - \frac{1}{r}(1 + 2p\frac{\partial}{\partial p})F_L^2 - \frac{2}{r}p\frac{\partial}{\partial p}\Delta G_L^1 - m(K\Delta G_R^1 + H\Delta F_R^1) - \Delta m(KG_R^1 + HF_R^1), \quad (43)$$

$$0 = \omega\Delta F_L^2 + \Delta G_L^{2'} - \frac{1}{r}(1 + 2p\frac{\partial}{\partial p})\Delta G_L^2 + \frac{2}{r}\frac{\partial}{\partial p}F_L^1 - m(K\Delta G_R^2 + H\Delta F_R^2) - \Delta m(KG_R^2 + HF_R^2), \quad (44)$$

$$0 = \omega G_L^1 - F_L^{1'} - \frac{1}{r}(2 + 2p\frac{\partial}{\partial p})F_L^1 + \frac{1}{r}(1 + 2p\frac{\partial}{\partial p})\Delta G_L^2 - m(HG_R^1 + KF_R^1) - \Delta m(H\Delta G_R^1 + K\Delta F_R^1) + 2pK(m\Delta G_R^2 + \Delta mG_R^2) + \frac{1-f_A}{r}(F_L^1 - p\Delta G_L^2) - \frac{f_B}{r}(G_L^1 + p\Delta F_L^2), \quad (45)$$

$$0 = \omega G_L^2 - F_L^{2'} - \frac{1}{r}(3 + 2p\frac{\partial}{\partial p})F_L^2 - \frac{2}{r}\frac{\partial}{\partial p}\Delta G_L^1 - m(HG_R^2 + KF_R^2) - \Delta m(H\Delta G_R^2 + K\Delta F_R^2) - 2K(m\Delta G_R^1 + \Delta mG_R^1) + \frac{1-f_A}{r}(F_L^2 + \Delta G_L^1) + \frac{f_B}{r}(-G_L^2 + \Delta F_L^1), \quad (46)$$

$$0 = \omega\Delta G_L^1 - \Delta F_L^{1'} - \frac{1}{r}(2 + 2p\frac{\partial}{\partial p})\Delta F_L^1 + \frac{1}{r}(1 + 2p\frac{\partial}{\partial p})G_L^2 - \Delta m(HG_R^1 - KF_R^1) - m(H\Delta G_R^1 - K\Delta F_R^1), \quad (47)$$

$$0 = \omega\Delta G_L^2 - \Delta F_L^{2'} - \frac{1}{r}(3 + 2p\frac{\partial}{\partial p})\Delta F_L^2 - \frac{2}{r}\frac{\partial}{\partial p}G_L^1 - \Delta m(HG_R^2 - KF_R^2) - m(H\Delta G_R^2 - K\Delta F_R^2). \quad (48)$$

These equations are analogous in structure to the equations in the sphaleron background, with all relevant features ‘doubled’. Now six equations contain p -dependent

terms (apart from the terms containing partial derivatives with respect to p). These are eqs. (33), (35), (37), (39), (41) and (45). And six functions occur with a prefactor p , these are $F_R^2, \Delta F_R^2, \Delta F_L^2, G_R^2, \Delta G_R^2$ and ΔG_L^2 , the six ‘bad’ functions, b . The other ten functions are the ‘good’ functions, g . Again, if the bad functions are small, all functions have little angular dependence, and an approximation with radial functions only will be good.

Let us therefore inspect the two source terms for the bad functions,

$$s_1 = HG_L^2 - KF_L^2 - 2K\Delta G_L^1, \quad (49)$$

$$s_2 = KG_L^2 + HF_L^2 - 2K\Delta F_L^1, \quad (50)$$

occurring in eqs. (38), (40), and in (34), (36), respectively, and split these two source terms according to $s_1 = a_1 - a_2$, with

$$a_1 = HG_L^2 - KF_L^2, \quad (51)$$

$$a_2 = 2K\Delta G_L^1, \quad (52)$$

and $s_2 = b_1 - b_2$, with

$$b_1 = KG_L^2 + HF_L^2, \quad (53)$$

$$b_2 = 2K\Delta F_L^1. \quad (54)$$

If both source terms are small, then the bad functions are small, and consequently the angular dependence of all 16 fermion functions is small.

Due to its great complexity, we have not yet attempted to solve the full set of 16 coupled partial differential equations numerically. Instead we have from the beginning resorted to the study of the approximate set of 16 ordinary differential equations, obtained by integrating out the angular dependence in the energy density. But even this approximate set of 16 ordinary differential equations has resisted a numerical solution along the full sphaleron barrier. Only by setting two of the 16 radial functions explicitly to zero, namely the supposedly small bad functions ΔG_L^2 and ΔG_R^2 , we have succeeded in constructing the fermion solution along the sphaleron barrier. (Note, that ΔG_L^2 has no source term.)

Without the solution of the partial differential equations to compare with, the quality of the approximate solution is not known along the full barrier, away from the sphaleron. At the sphaleron the approximation is excellent, and it should remain good close to the sphaleron. Away from the sphaleron, however, we can at least make a consistency check for the radial approximation used, by inspecting the source terms s_1 and s_2 in this approximation. Numerical analysis shows, that the source terms are indeed small. In Fig. 7 we show as a typical example along the barrier the source terms b_1 and b_2 for the Chern-Simons number $N_{CS} = 0.4$ and the mass parameters $m = 0.5$ and $\Delta m = 0.25$. While the cancellation of the source terms a_1 and a_2 remains as good along the barrier as it is at the sphaleron (shown in Fig. 6), the cancellation of the additional source terms b_1 and b_2 is even much better. This indicates, that the bad functions are indeed small compared

to the good functions. The radial approximation therefore should be good along the full sphaleron barrier.

Let us then discuss the level crossing along the sphaleron barrier, as obtained with the approximate radial set of equations. In Fig. 8 we present the fermion eigenvalue along the barrier for an average mass of $m = 2$ and for several values of the mass difference, $\Delta m = 0.5, 1.0$ and 1.5 . The eigenvalue starts from the positive continuum at the lower mass ($1.5, 1.0$ and 0.5 , respectively), and reaches the negative continuum at the corresponding negative value. The bigger the mass splitting, i.e. the smaller the lower mass, the later the fermion level leaves the continuum to become bound, analogous to the case of degenerate fermion masses [14,15,20].

For degenerate fermion masses the fermion wavefunction is determined by the hedgehog spinor χ_h , giving both isospin components of the fermion doublet an equal amplitude along the sphaleron barrier. For nondegenerate fermion masses this is no longer the case. Let us define the up-part of the fermion wavefunction along the barrier as

$$\frac{\langle P\Psi, P\Psi \rangle}{\langle \Psi, \Psi \rangle}, \quad (55)$$

where P projects out the upper isospin component. (Note, that this definition of the up-part is not gauge invariant.) For degenerate fermions the up-part is everywhere one half. For nondegenerate fermions the up-part along the barrier depends on the size of the mass splitting, as shown in Fig. 9 (for the mass parameters employed also in Fig. 8). The up-part dominates slightly in the vicinity of the sphaleron and clearly disappears when the vacua are reached. Remarkably, the point where the down-part equals the up-part only depends on m and not on Δm .

We finally address the question, how to best approximate a fermion solution in the physical situation of nondegenerate fermion masses by a far simpler solution, obtained in the approximation of degenerate fermion masses, in the vicinity of the sphaleron. In the physical case the mass parameters m and Δm determine the nondegenerate masses, $m + \Delta m$ and $m - \Delta m$. Close to the continuum clearly the lower mass, $m - \Delta m$, is the relevant fermion mass. In the vicinity of the sphaleron, however, it is the average mass m , which matters. In fact, the average mass m of the nondegenerate case mostly leads to an excellent approximation for the fermion eigenvalue in the vicinity of the sphaleron, when employed in the far simpler calculations with degenerate fermion mass. This is demonstrated in Fig. 10, where we compare the nondegenerate case $m = 2, \Delta m = 1$ with the degenerate cases $m = 1, \Delta m = 0$ and $m = 2, \Delta m = 0$. Having the same average mass, the fermion eigenvalues in the nondegenerate case, and in the second degenerate case, agree very well in the vicinity of the sphaleron. In Fig. 11 we present the slope of the fermion eigenvalue at the sphaleron as a function of the mass difference, for three values of the average mass, $m = 0.5, 1$ and 2 . We observe, that the slope is fairly independent of the mass difference Δm for not too large values of the average mass m .

6 Conclusion

We have considered level crossing in the background field of the sphaleron barrier for fermion doublets with nondegenerate masses. The mass splitting necessitates a generalized ansatz for the fermions, possessing only axial symmetry. We have proposed a particular parametrization of the axially symmetric ansatz, containing 16 real functions of the two variables r and $p = \cos^2 \theta$. The structure of the ansatz chosen is based on the structure of the spherically symmetric ansatz, which represents its simple limit for vanishing mass splitting. This particular parametrization has the great advantage, that it leads to fermion functions with little angular dependence in the background of the sphaleron, and (supposedly) also along the full sphaleron barrier.

In the background field of the sphaleron the proposed ansatz simplifies considerably. It leads to a set of eight partial differential equations. We have solved these equations numerically, finding that the resulting fermion functions have very little angular dependence. The reason lies in the structure of the equations for this particular choice of ansatz. Only three functions occur with an angular dependent prefactor p (apart from partial derivative terms), and there is a single source term for these three functions. Since this source term is small, these three functions, which introduce explicit angular dependence into the equations, are small, and consequently all eight functions have only little angular dependence.

We have then proposed an approximate ansatz with radial functions only. Integrating out the angular dependence in the energy density, leads to a new approximate set of ordinary differential equations. Solving these numerically, we find that the solutions are in excellent agreement with those of the full calculation. Thus we have an excellent radial approximation for nondegenerate fermion masses at the sphaleron.

In the general case of fermions in the background of the sphaleron barrier, we have found the same structure of the equations as in the sphaleron case, but with all relevant features ‘doubled’, since the ansatz no longer simplifies. As yet we have only solved the approximate set of ordinary differential equations, obtained by integrating out the angular dependence in the energy density (and then setting two of the small functions explicitly to zero). Without the solution of the set of partial differential equations to compare with, we do not know the quality of the approximation away from the sphaleron. However, we have made a consistency check by evaluating the two source terms for the six functions, which introduce explicit angular dependence into the equations. Since the source terms are small, these functions are small, and consequently all functions have only little angular dependence. We therefore argue, that the radial approximation employed should be good along the full barrier.

Considering level crossing along the barrier, we have observed that the fermion mode which crosses zero energy at the sphaleron reaches the continua at the lower fermion mass, as expected. Finally we have shown, that in the vicinity of the sphaleron the eigenvalue for nondegenerate fermions with average mass m and mass difference Δm , may be well approximated by the eigenvalue obtained with the far simpler calculation, involving only degenerate fermions with the average mass m . With respect to the large splitting of the

top and bottom quark masses, this suggests to rather use half the top quark mass in approximate calculations with degenerate fermions.

References

- [1] A. D. Sakharow, JETP Letters 5 (1967) 5
- [2] G. 't Hooft, Symmetry breaking through Bell-Jackiw Anomalies, Phys. Rev. Lett. 37 (1976) 8.
- [3] N. S. Manton, Topology in the Weinberg-Salam theory, Phys. Rev. D28 (1983) 2019.
- [4] F. R. Klinkhamer, and N. S. Manton, A saddle-point solution in the Weinberg-Salam theory, Phys. Rev. D30 (1984) 2212.
- [5] A. Ringwald, Rate of anomalous electroweak baryon and lepton number violation at finite temperature, Phys. Lett. B201 (1988) 510.
- [6] M. Mattis, and E. Mottola, eds., “Baryon Number Violation at the SSC?”, World Scientific, Singapore (1990).
- [7] P. Arnold, and L. McLerran, Sphalerons, small fluctuations, and baryon-number violation in electroweak theory, Phys. Rev. D36 (1987) 581.
- [8] P. Arnold, and L. McLerran, The sphaleron strikes back: A response to objections to the sphaleron approximation, Phys. Rev. D37 (1988) 1020.
- [9] L. Carson, X. Li, L. McLerran, and R.-T. Wang, Exact computation of the small-fluctuation determinant around a sphaleron, Phys. Rev. D42 (1990) 2127.
- [10] E. W. Kolb, and M. S. Turner, “The Early Universe”, Addison-Wesley Publishing Company, Redwood City (1990).
- [11] C. R. Nohl, Bound-state solutions of the Dirac equation in extended hadron models, Phys. Rev. D12 (1975) 1840.
- [12] J. Boguta, and J. Kunz, Hadroids and sphalerons, Phys. Lett. B154 (1985) 407.
- [13] A. Ringwald, Sphaleron and level crossing, Phys. Lett. B213 (1988) 61.
- [14] J. Kunz, and Y. Brihaye, Fermions in the background of the sphaleron barrier, Phys. Lett. B304 (1993) 141.
- [15] J. Kunz, and Y. Brihaye, Level crossing along sphaleron barriers, Phys. Rev. D50 (1994) 1051.

- [16] D. Diakonov, M. Polyakov, P. Sieber, J. Schaldach, and K. Goeke, Fermion sea along the sphaleron barrier, Phys. Rev. D49 (1994) 6864.
- [17] B. Kleihaus, J. Kunz, and Y. Brihaye, The electroweak sphaleron at physical mixing angle, Phys. Lett. B273 (1991) 100.
- [18] J. Kunz, B. Kleihaus, and Y. Brihaye, Sphalerons at finite mixing angle, Phys. Rev. D46 (1992) 3587.
- [19] B. Kastening, Fermionic instanton zero modes in models with spontaneous symmetry breaking and broken custodial SU(2) symmetry, Phys. Lett. B291 (1992) 92.
- [20] G. Nolte, and J. Kunz, Gradient approach to the sphaleron barrier, Phys. Rev. D51 (1995) 3061.

Sphaleron

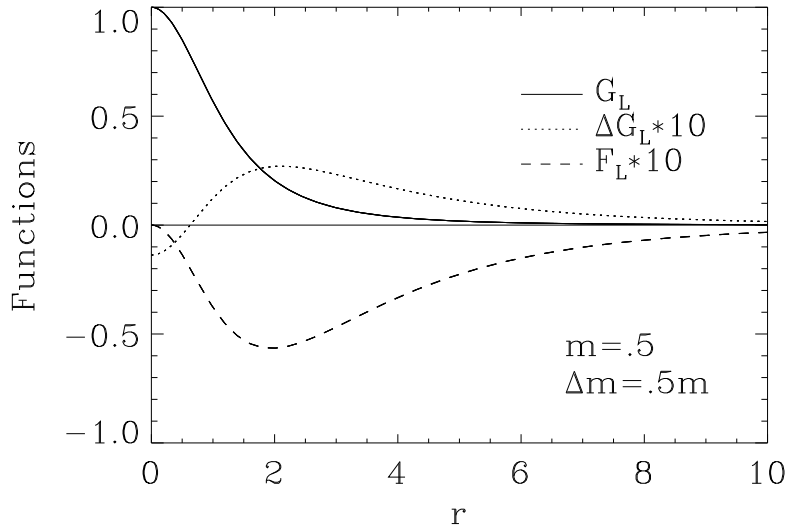


Figure 1: The ‘good’ lefthanded functions, G_L (solid), ΔG_L (dotted) and F_L (dashed), in the background field of the sphaleron with normalization $G_L(0) = 1$, in the exact calculation for three values of the angle θ ($\theta = 0, \pi/4$ and $\pi/2$) and in the approximate calculation, with the mass parameters $m = 0.5$ and $\Delta m = 0.25$. Any of the three visible lines consists of four individual lines.

Sphaleron

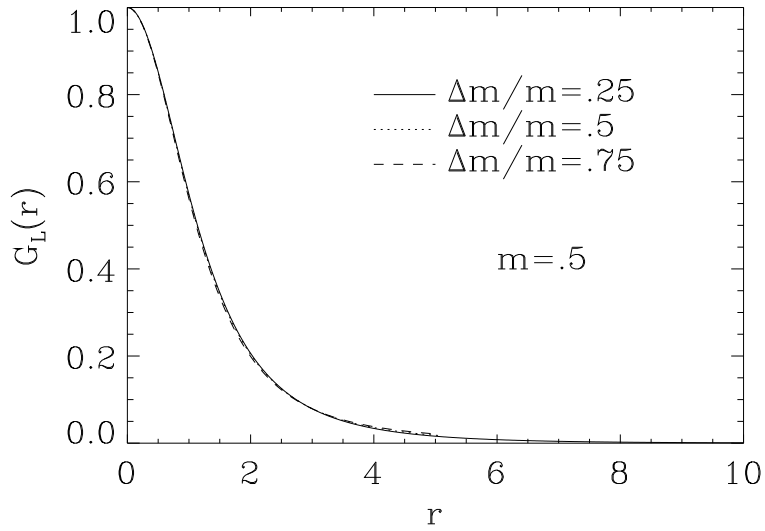


Figure 2: The ‘good’ lefthanded function G_L in the background field of the sphaleron in the approximate calculation, for the fixed average mass $m = 0.5$ and three values of the mass difference $\Delta m = 0.25$ (solid), $\Delta m = 0.50$ (dotted), $\Delta m = 0.75$ (dashed).

Sphaleron

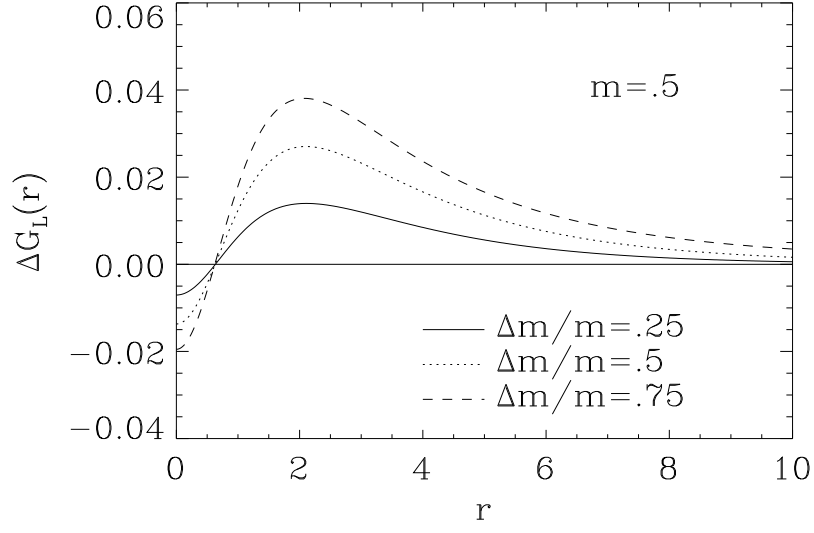


Figure 3: Same as Fig. 2 for ΔG_L .

Sphaleron

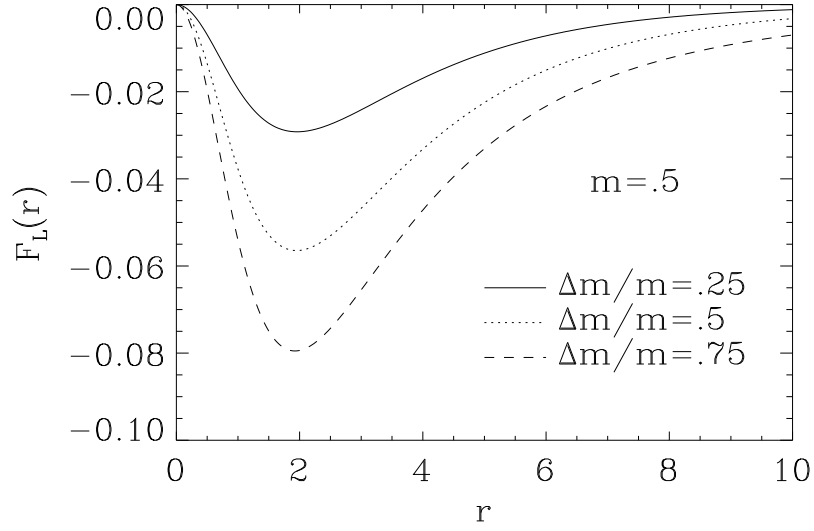


Figure 4: Same as Fig. 2 for F_L .

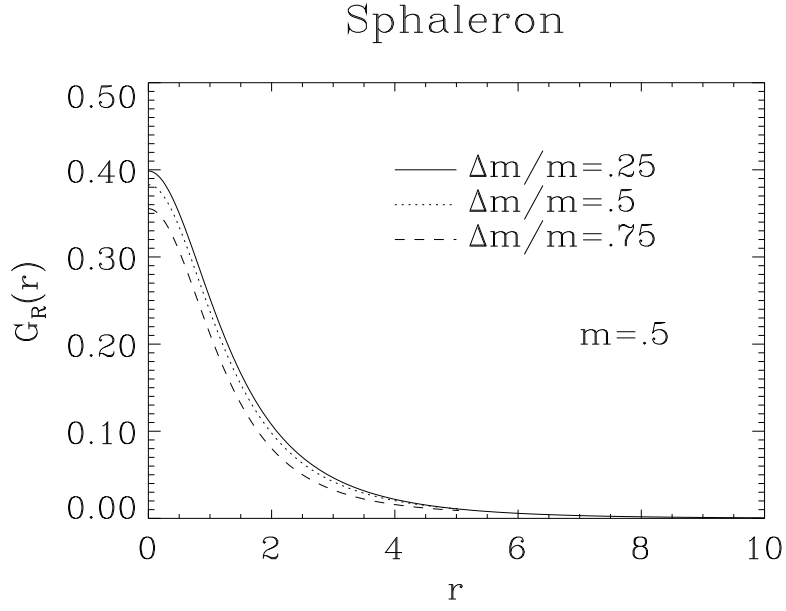


Figure 5: Same as Fig. 2 for G_R .

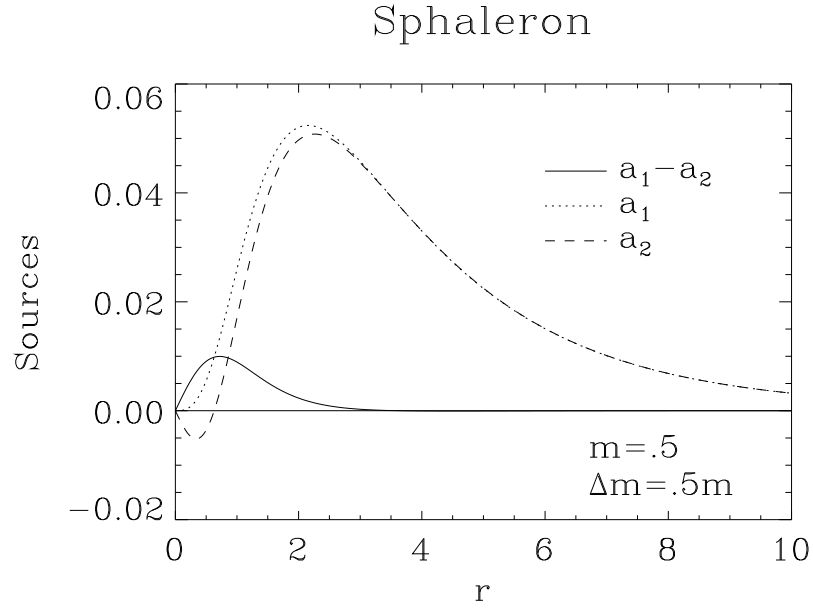


Figure 6: The source term $s = a_1 - a_2$ (solid), and its individual parts a_1 (dotted) and a_2 (dashed) in the background field of the sphaleron in the approximate calculation, with the mass parameters $m = 0.5$ and $\Delta m = 0.25$.

Barrier

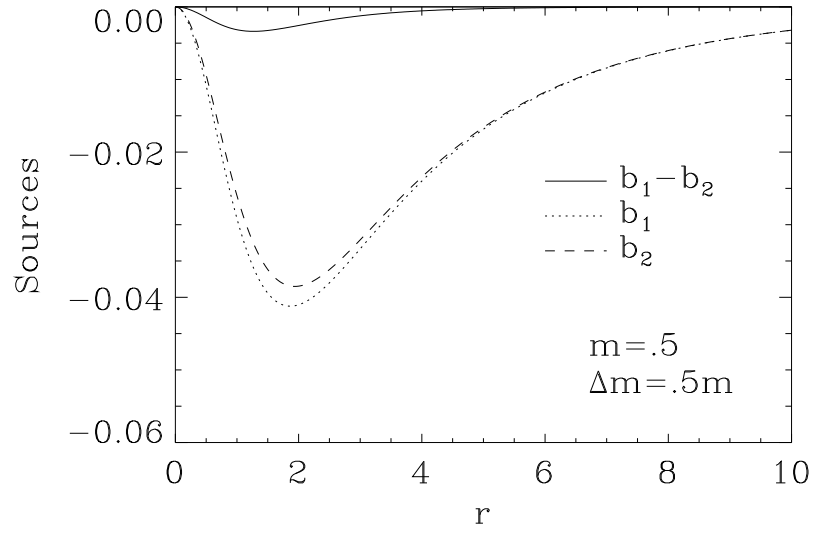


Figure 7: The source term $s_2 = b_1 - b_2$ (solid), and its individual parts b_1 (dotted) and b_2 (dashed) in the background field of the sphaleron barrier at the Chern-Simons number $N_{CS} = 0.4$ in the approximate calculation, with the mass parameters $m = 0.5$ and $\Delta m = 0.25$.

Barrier

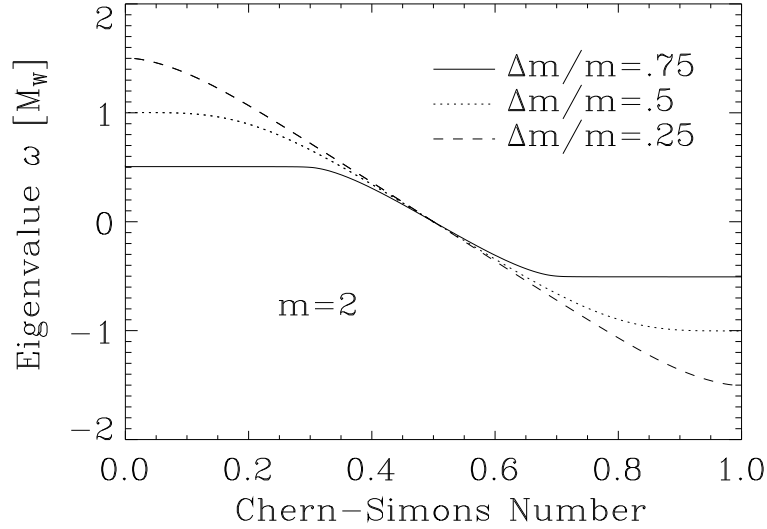


Figure 8: The fermion eigenvalue along the sphaleron barrier in the approximate calculation, for the fixed average mass $m = 2$ and three values of the mass difference $\Delta m = 0.75$ (solid), $\Delta m = 0.50$ (dotted), $\Delta m = 0.25$ (dashed).

Barrier

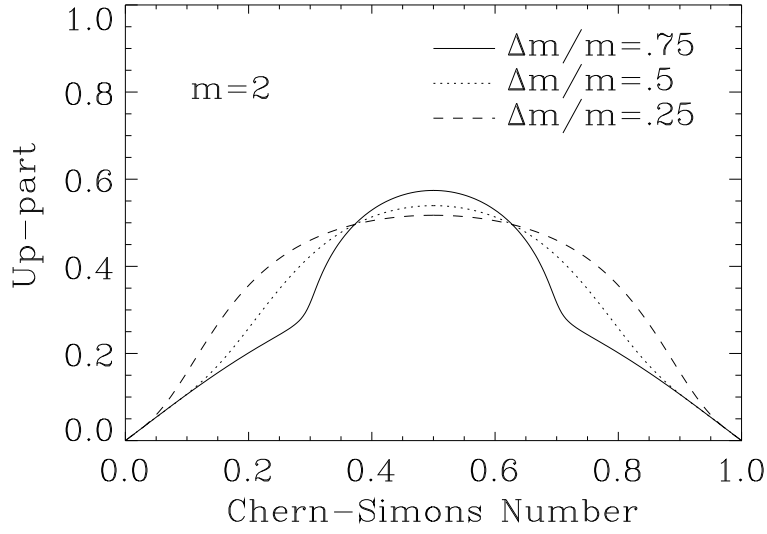


Figure 9: The up-part of the fermion wavefunction along the sphaleron barrier in the approximate calculation, for the fixed average mass $m = 2$ and three values of the mass difference $\Delta m = 0.75$ (solid), $\Delta m = 0.50$ (dotted), $\Delta m = 0.25$ (dashed).

Barrier

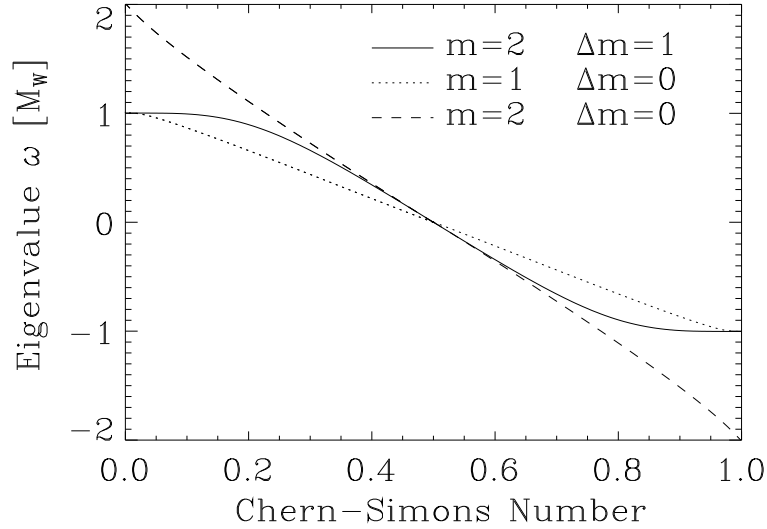


Figure 10: The fermion eigenvalue along the sphaleron barrier in the approximate calculation for the average mass $m = 2$ and the mass difference $\Delta m = 1$ (solid), compared to the fermion eigenvalue for degenerate fermion masses for $m = 1$ and $\Delta m = 0$ (dotted), and $m = 2$ and $\Delta m = 0$ (dashed).

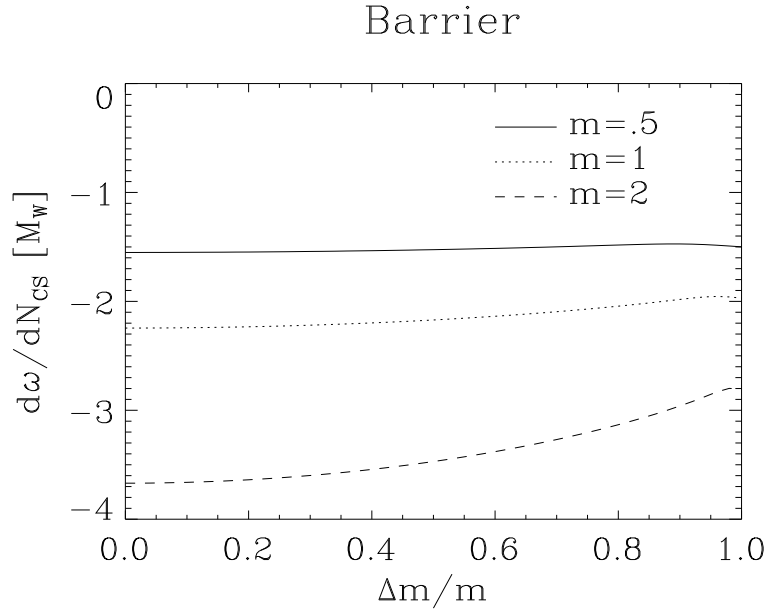


Figure 11: The slope of the fermion eigenvalue at the sphaleron in the approximate calculation, as a function of the mass difference Δm for three values of the average mass, $m = 0.5$ (solid), $m = 1$ (dotted), $m = 2$ (dashed).